Eur. Phys. J. D (2015) 69: 284
DOI: 10.1140/epjd/e2015-60458-y

THE EUROPEAN PHYSICAL JOURNAL D

Regular Article

Double-pulse induced harmonic generation in laser-produced plasmas

Rashid A. Ganeev[a], Masayuki Suzuki, Shin Yoneya, and Hiroto Kuroda

Ophthalmology and Advanced Laser Medical Center, Saitama Medical University, Saitama 350-0495, Japan

Received 5 August 2015 / Received in final form 8 November 2015
Published online 17 December 2015 –

Abstract. We report the studies of the metals, non-metals, powders, and nanoparticles as the targets for laser ablation induced high-order harmonic generation of ultrashort pulses using the double-pulse technique. The proposed technique demonstrates the attractiveness as the method for the studies of the high-order nonlinear optical properties of various materials. The comparative analysis of the harmonic generation using different targets showed that the species allowing easier ablation (powders, nanoparticles) produce stronger harmonic yield in the extreme ultraviolet range.

1 Introduction

The analysis of the physical properties of matter using the nonlinear optical methods has long been considered as one of the attractive methods of material science [1–5]. In the visible spectral range, this method was realized by propagation of the strong ultrashort pulses through the transparent solid (or liquid) media, which led in some cases to the low-order harmonic generation. Solid medium can cause the high-order harmonic generation (HHG) as well once the problem of absorption of the generated radiation will be solved. A search for new methods of the HHG in solid targets led to the studies [6,7], which defined the main principles of this technique. Though some applications of mid-infrared lasers led to the HHG in solids [8] covering the longer wavelength region, a strong absorption of any material in the spectral region below 105 nm did not allow the application of solid-like dense media for the HHG in the extreme ultraviolet (XUV) range (10−100 nm).

The straight way for analysis of the high-order nonlinear optical properties of matter in the XUV range is a decrease of medium density, which allows diminishing the material breakdown by intense pulses, as well as the re-absorption of harmonic emission. The plasma harmonic approach [9] is an example of the nonlinear optical spectroscopy of ablated solids using the analysis of the high-order nonlinear optical properties of the low-density plasmas produced on the surfaces of these media. In that case, notably lower density of plasmas compared with solids ($\sim 10^{17}$ and $\sim 10^{23}$ cm^{-3} respectively) allows significantly diminish the optical breakdown and absorption processes during HHG in such media. In accordance with conventional approach for harmonic generation in laser-produced plasmas, the fundamental ultrashort pulses are properly delayed compared with the heating picosecond pulses to allow the formation of the optimal plasma on the path of the fundamental beam. To apply this technique, two (femtosecond and picosecond) pulses should be separated by a few tens nanoseconds from each other. In most cases, this method allows the observation of various interesting processes in the ablated materials (e.g. resonance enhancement of single harmonic, nanoparticle and two-color pump induced growth of harmonic yield, to mention few of them). However, while offering a variety of options, this method lacks robustness in preparation of the optimal plasma for the HHG.

Recently, we have proposed the method of harmonic generation using the two femtosecond pulses sequentially propagating in the vicinity of targets, without preliminary ablation of the surface by picosecond heating pulse (double-pulse method [10]). The efficiency and cut-off of harmonic generation using the double-pulse method in most cases were lower compared with the commonly used method of plasma harmonics generation. At the same time, a simplicity, absence of additional source of heating radiation, and artificial optimization of the HHG using the spatial and temporal adjustment of the double pulses and targets have shown the advantages of this technique, which allow the characterization of the high-order nonlinear optical properties of the media using a significantly simplified conditions of experiments.

In present paper, we analyze the application of this double-pulse method for the studies of the nonlinear optical properties of the plasmas produced during ablation of various extended targets comprising the metals, nonmetals, micro-powders, and nanoparticles. The proposed technique proved to be useful for both the simplification of harmonic generation in the XUV region, amendment of harmonic yield compared with above approach, and the analysis of the optical nonlinearities of various materials.

[a] e-mail: rashid_ganeev@mail.ru

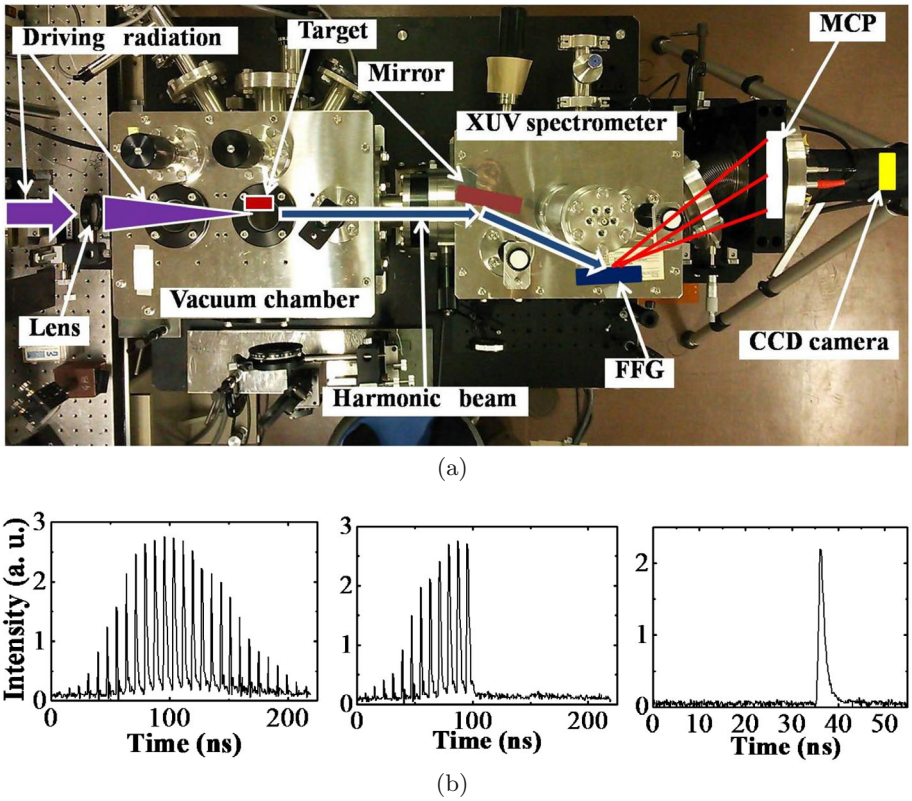

Fig. 1. (a) Image of double-pulse experiments. FFG, flat field grating; MCP, microchannel plate. (b) Oscilloscope traces of the pulse train generated in the regenerative amplifier (left panel), remaining part of train after separation of the single pulse from the central part of this train (central panel), and single pulse (right panel).

2 Experimental arrangements

The radiation of Ti:sapphire laser (central wavelength 802 nm, pulse duration 70 fs, pulse energy 4 mJ, 10 Hz pulse repetition rate) was focused using the 400 mm focal length spherical lens and propagated close to the targets placed in the vacuum chamber (Fig. 1a). The intensity of single driving pulse at the focus area was 8×10^{14} W cm^{-2}. The targets (5-mm-long metals, non-metals, powders, and nanoparticles) moved towards the optical axis of the fundamental beam to create the conditions when the focusing radiation "touches" and ablates the targets by its wings of spatial distribution. We estimated the average intensity on the ablating surface at optimal conditions of harmonic generation to be 5×10^{9} W cm^{-2}, assuming the ratio of interacting beam, which touched the surface. The extreme ultraviolet spectrometer was used for analysis of plasma and harmonic emission and consisted on cylindrical mirror, flat field grating, microchannel plate and CCD camera (Fig. 1a). In the case of single femtosecond pulse, the only emission in the short-wavelength range was the one from plasma plume observed at the conditions when the targets were moved closer to the optical axis of laser beam, which led to increase of laser intensity on the target surface ($>10^{10}$ W cm^{-2}) and strong ablation.

The conditions of plasma formation and laser-plasma interaction were dramatically changed once we introduced the double-pulse scheme. The double-pulse beam was produced by tuning the triggering signal on the Pockels cell of the regenerative amplifier (TSA-10, Spectra-Physics Lasers) of Ti:sapphire laser. Usually, this Pockels cell was used for separation of a single pulse from the train of the pulses generated in the regenerative amplifier (Fig. 1b). The tuning of the triggering signal of Pockels cell allowed separation of the two pulses with the 8 ns time interval, instead of the single pulse separation. We were able producing two pulses with variable ratio of the intensities of these pulses.

Exact beam geometry in the vicinity of targets is presented below. The confocal parameter of focused radiation (12 mm) was larger than the length of targets (5 mm). Correspondingly the intensity of the part of focused beam interacting with target was the same along the whole range of propagation of driving beam near the target. This intensity was varied depending on the properties of targets in the range of 2×10^{9} W cm^{-2} to 8×10^{9} W cm^{-2}. The scheme of laser-matter interaction at these conditions is shown in Figure 2a. The wing of the first beam touches and ablates target surface and the second beam propagates through the area filled with the ablated material. Panel 1 of Figure 2b shows the conditions similar to the right panel of Figure 1b, when the single pulse was separated from the train. It also demonstrates the reasonably high contrast of the main pulse with regard to other pulses

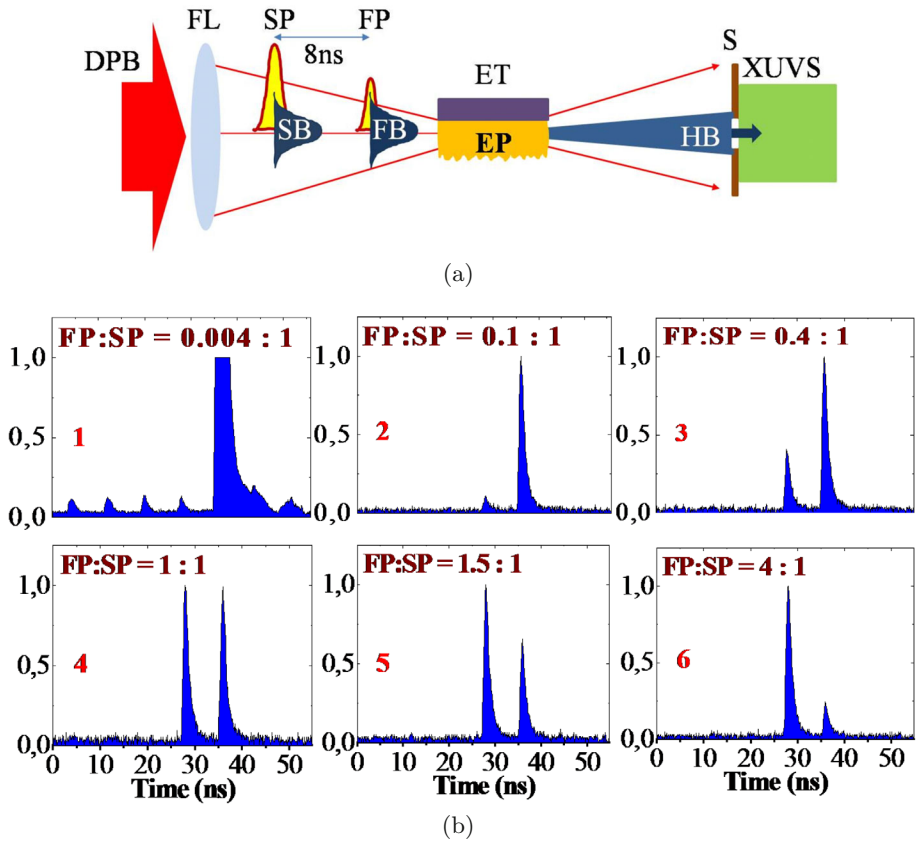

Fig. 2. (a) Experimental arrangements for harmonic generation during ablation of various targets by the wing of the spatial distribution of the first beam using the double-pulse scheme. DPB, double-pulse beam; FL, focusing lens; FP, first pulse; SP, second pulse; FB, first beam; SB, second beam; ET, extended target; EP, extended plasma; HB, harmonic beam; S, slit; XUVS, extreme ultraviolet spectrometer. (b) Oscilloscope traces of double pulses at different ratios of the first and second pulses.

of the train. The ratio of pre-pulses and main pulse in that case was 4×10^{-3}. The intensity of these weak pre-pulses did not allow plasma formation during interaction of the wings of spatial distribution and the surfaces of targets. It means that no plasma was formed prior to propagation of the single pulse. This single pulse itself caused the target ablation, which resulted in the incoherent plasma emission, as was described above.

Once we gradually changed the delay of the triggering pulse on the Pockels cell, the neighboring pre-pulse with variable intensity was appeared on the oscilloscope trace, alongside with the main pulse. We tuned the ratio the first pulse (FP) and second pulse (SP) intensities between 0.1:1 to 4:1 (Fig. 2b, panels 2−6). At these conditions, the dynamics of laser-matter interaction was significantly changed compared with the above-described case of single pulse interaction. First pulse (for example, panel 2 of Fig. 2b), with the intensity ten times smaller compared with the second pulse, created the plasma plume during ablation of the target surface by the wings of the spatial distribution of this first beam (FB, Fig. 2a). The ablated species along the whole target moved toward the optical axis of the laser beam propagation. The second beam (SB) propagated, 8 ns later, through the area where some fastest particles of plasma had appeared. This interaction of the second pulse with the ablated species resulted in harmonic generation. The tuning of the distance between the target and laser beam (d) allowed choosing the conditions when the generating harmonics prevail over the plasma emission. The optimal distance (d_{opt}) was varied for different targets under consideration. Solid metal targets were used at less distance between the target surface and the optical axis, since those solids required relatively high intensities of the first pulse for the surface ablation. Contrary to that, the "mild" solids, such as organic species and glued micro- and nanoparticles, were ablated at less intensity of the laser pulse resulting in larger values of d_{opt}.

3 Results and discussion

The application of 5-mm-long solid silver target allowed harmonic generation only at the large ratios of FP:SP corresponding to the small d_{opt} (60−80 μm). Two upper panels of Figure 3a show the harmonic spectra obtained at 1:1 and 2:1 ratios of the first and second pulses. We compared these double-pulse induced harmonic spectra with

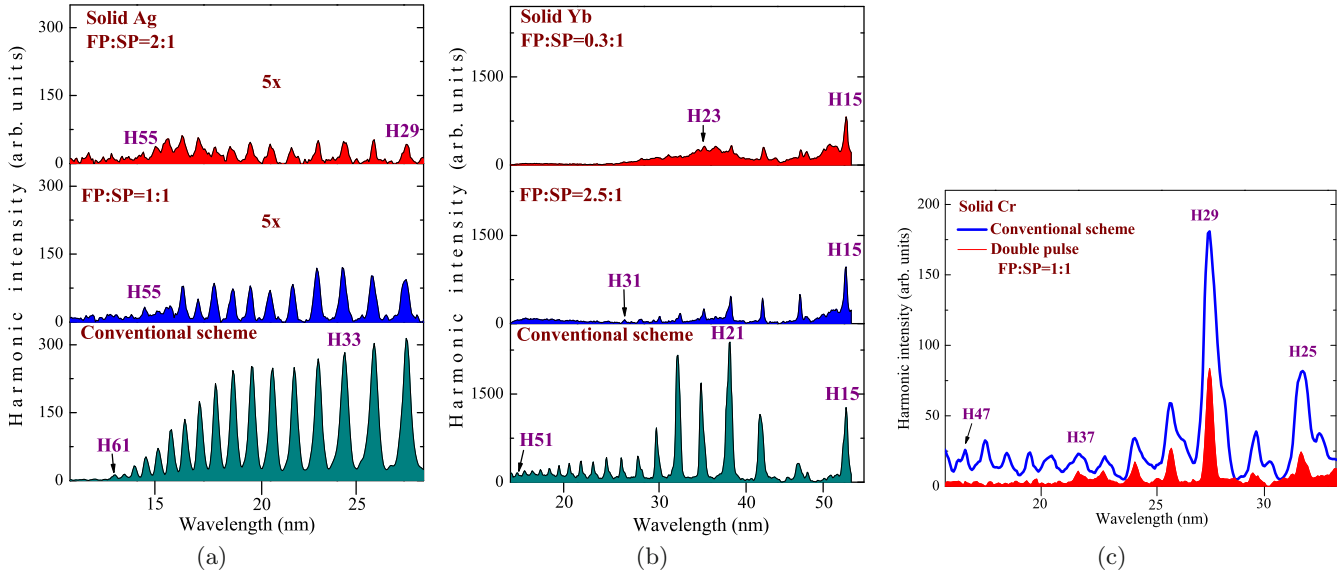

Fig. 3. Harmonic spectra in the cases of double-pulse and conventional schemes of plasma harmonic generation using the solid metal targets (see text). (a) Ag, (b) Yb, (c) Cr.

the conventional scheme of harmonic generation in the laser-produced plasma. In the latter case, we used the uncompressed pulses (t = 370 ps) from the same laser for the plasma formation. These heating pulses were focused using a 200 mm focal length cylindrical lens inside the vacuum chamber containing an ablating target to create the extended plasma plume. The single driving compressed pulse (t = 70 fs) was used, 45 ns from the beginning of ablation, for harmonic generation in the plasma plume. This delay between picosecond and femtosecond pulses allowed the achievement of highest harmonic yield. The driving pulse was focused onto the prepared extended plasma from the orthogonal direction, at a distance of ~150 μm above the target surface. The harmonic cut-off using double-pulse scheme was insignificantly lesser compared with the conventional plasma HHG approach (H55 and H61 respectively; compare second and third panels of Fig. 3a). The harmonic spectra presented in the case of double-pulse scheme (two upper panels) were multiplied with the factor of 5× for better visibility and comparison with the bottom panel, which shows the harmonic distribution generated using the conventional scheme. The harmonic yields in the former cases were 10 to 15 times lower compared with the conventional approach of plasma harmonic generation. The conversion efficiencies were defined to be 1×10^{-6} and 1.5×10^{-5} using double-pulse and conventional schemes respectively.

The harmonics using the ablation of solid ytterbium target (Fig. 3b) also showed stronger yield only in the case of relatively high ratios of the FP and SP intensities (2.5:1, central panel). At smaller ratio, the process of HHG was less efficient and required the placement of the target as close as possible to the axis of laser beam propagation. In that case, incoherent plasma emission was prevailed over harmonics (upper panel). The harmonic cut-off (H31) at optimal conditions (FP:SP = 2.5:1) was notably smaller compared with the conventional scheme of harmonic generation from ytterbium plasma (H71, not shown in the bottom panel; the cut-off in that case was defined by moving the micro-channel plate of XUV spectrometer towards the shorter wavelength region in the separate set of experiments).

The application of conventional scheme in the case of chromium target showed a pronounced 29th harmonic, which was stronger compared with the neighboring orders (Fig. 3c, upper solid curve). The enhancement of single harmonic from this plasma has been earlier attributed to the influence of the strong ionic transitions of ablated material in the vicinity of 29th harmonic (wavelength λ = 27.66 nm; photon energy $E_{\rm ph}$ = 44.83 eV) [11]. This harmonic was approximately coincided with the short-wavelength wing of the strong spectral band of the $3p \rightarrow 3d$ transitions of Cr II ions. Previous studies of the photoabsorption and photoionization spectra of Cr plasma in this XUV region have demonstrated the strong transitions [12–14], which could be responsible for such a heterogeneous pattern of harmonic spectrum. In particular, the region of the "giant" $3p \rightarrow 3d$ resonances of Cr II spectra was analyzed in reference [14]. The strong transitions, which could both enhance and diminish the nonlinear optical response of chromium, were revealed. The calculations of the oscillator strength (gf) in the photon energy range of 40–60 eV presented in reference [12] have shown a group of transitions in the 44.5–44.8 eV region possessing very strong oscillator strengths (with gf varying between 1 and 2.2), which considerably exceeded those of other transitions in the 20–40 nm spectral range. These transitions were assumed to be responsible for the observed enhancement of the 29th harmonic. At the same time, the strong photoabsorption lines within the 41–42 eV region reported

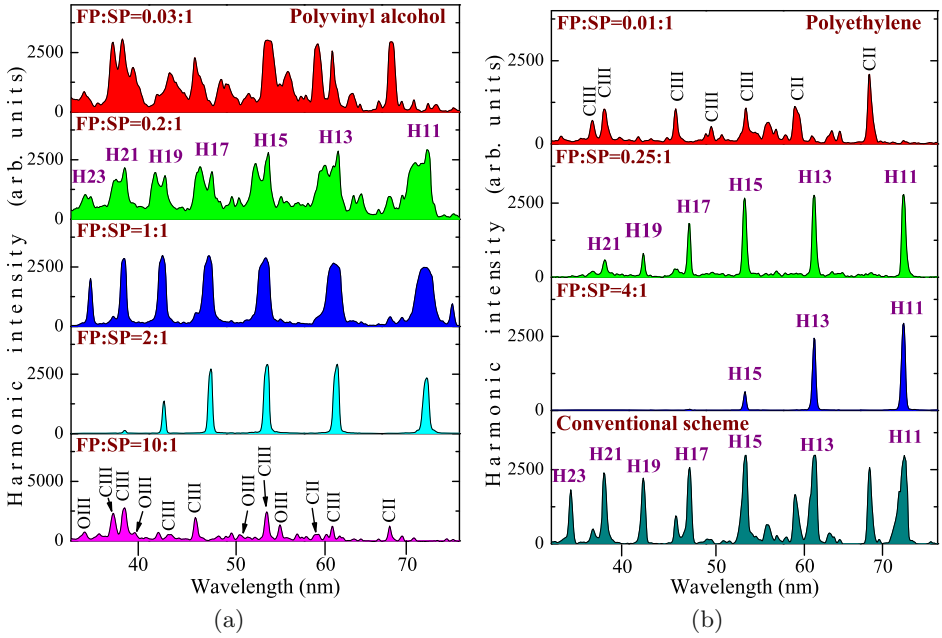

Fig. 4. Harmonic and plasma emission spectra in the cases of double-pulse and conventional schemes applied to the (a) polyvinyl alcohol and (b) polyethylene solid targets.

in the above work could decrease the yield of the 27th harmonic ($\lambda = 29.7$ nm; $E_{\rm ph} = 41.74$ eV) observed in our study (Fig. 3c).

Here we also show the spectrum of harmonics (red filled curve) obtained in the case of double-pulse scheme at the optimal FP:SP ratio (1:1). While being less intense and less extended, this spectrum shows similar features characterizing the ablated chromium species, particularly the enhancement of H29 and suppression of H27. Thus the proposed method allows the analysis of resonance-induced modification of the high-order nonlinear optical response of ablated medium using the significantly simplified experimental arrangement.

Another group of solids comprised the polymer-based species. The polyvinyl alcohol $(C_2H_4O)_n$ and polyethylene $(C_2H_4)_n$ showed the stronger yields of harmonics in the case of lesser FP:SP ratios compared with the metal targets. The reason of the change of the optimal ratio between two pulses was the easier ablation of solid organic polymers compared with the solid metals. Whilst in most cases this ratio for solid metals was in the range of 3:1–1:1, the HHG in the vicinity of polymers was optimized at lesser intensity of the first pulse compared with the second one. The conversion efficiency towards the higher-order harmonics generated in polyvinyl alcohol (PVA) and polyethylene (PE) using double-pulse method was eight times weaker compared with the conventional scheme, while the lower orders (H15, H17) showed approximately similar intensities in these two cases. Below we analyze some peculiarities observed during studies of the emission spectra from the PVA and PE plasmas.

Figure 4a shows the harmonic spectra obtained in the case of PVA target using the variable values of FP:SP ratio. At very small FP:SP ratio (0.03:1, upper panel), no harmonics were generated with the decrease of d, until the conditions when strong plasma emission became dominated in the observed spectrum. The spectral lines of this emission were assigned to the singly and (mostly) doubly ionized carbon and oxygen (see also bottom panel). The growth of FP:SP ratio allowed defining the conditions when very strong broadband harmonics up to the 23rd order became dominated, alongside with plasma emission, in the observed spectra (FP:SP = 0.2:1, second panel).

The characteristic feature of this spectrum is the appearance of the short-wavelength lobes close to each harmonic order. In some cases, they were stronger than the harmonics (H15–H19; Fig. 4a, second panel). Broader widths of harmonics caused by addition of the shorter-wavelength lobes can be explained by self-phase modulation (SPM) and chirping of the fundamental radiation propagating through the plasma. Broadening of the fundamental beam bandwidth causes the broadening of the harmonic bandwidth. In the case of SPM in laser plasma, one can expect a considerable variation of the harmonic spectrum compared with the case of moderate intensities of laser radiation, when no change in spectrum of the fundamental or harmonic radiation is expected. In our studies, the extension of harmonic spectral distribution toward the blue side was observed, which shows that, in the case of some plasmas, one can expect a considerable SPM and corresponding modulation of the harmonic spectrum.

Further growth of FP:SP ratio led to the appearance of the "clean" harmonics, without the lobes (1:1, third panel), which then were decreased (at 2:1 ratio, fourth panel), and finally disappeared from the spectra (at 10:1 ratio, bottom panel). In the latter case, the plasma

spectrum was observed similar to the one shown in the upper panel, when very small FP:SP ratio was used, which point out the formation of similar unfavorable conditions for harmonic generation.

Similar dynamics of spectral variations was observed in the case of PE (Fig. 4b). Strong emission mostly attributed to the C III ions was generated at FP:SP = 0.01:1 (upper panel). Maximal harmonic yield and cut-off were obtained at 0.25:1 ratio (up to H21; second panel). We compared these spectra with the one observed during conventional plasma HHG (bottom panel). In the latter case, the harmonic cut-off was H39 (not shown in this panel). One can see the emission of C III ions, alongside with harmonic emission. The presence of singly and doubly charged carbon ions and correspondingly some amount of free electrons did not prevent the harmonic generation since the concentration of these electrons was significantly lower than the ones produced during tunnel ionization of plasma species by single femtosecond pulse. Note that in both PVA and PE (Fig. 4a, bottom panel and Fig. 4b, upper panel) similar C III lines in the XUV range were appeared.

We also generated harmonics using the double-pulse technique in graphite bulk target. The double-pulse method allowed generation of weak lower-order harmonics using this target. The plasma emission from ablation of this target was considerably stronger than the higher-order harmonic emission. In the meantime, application of the conventional method based on the preliminary ablation of graphite by 370 ps pulses followed with the delayed propagation of the 70 fs single pulses through the optimally formed plasma led to very strong lower-order harmonic generation, with the conversion efficiency estimated to be $\sim 6 \times 10^{-5}$, similarly to those reported in previous study [15]. Probably, in the case of graphite target, the conditions of plasma formation during interaction of the spatial wing of the first beam with the target surface did not produce a sufficient amount of carbon particles in the interaction zone.

Multiatomic particles subject to intense laser pulses produce strong low-order nonlinear optical response (e.g. nonlinear refraction and nonlinear absorption), as well as can emit coherent XUV radiation through HHG [16–19]. There many powdered species exist in the form of microparticles. This set of our studies was related with the microparticle- and nanoparticle-induced HHG using double-pulse method. Firstly, we analyzed the microparticle powders of the products of common use (sugar and coffee powders with the sizes of particles of the order of a few ten to a few hundred micrometers) using the double-pulse scheme to define the difference of the harmonic yields from the species of different consistency and dimensions. The powders of above species were glued on the 5-mm-long glass substrates and further used as the targets for double-pulse induced HHG. These studies were also carried out at different ratios of the first and second pulses of the driving radiation. Some advantages of the microparticles over nanoparticles were observed with the stronger harmonic yield in the former case (see also the final stage of these studies). A peculiarity of observed harmonic spectra in the cases of sugar and coffee microparticles was related with the broad range of FP:SP ratios at which the "clear" spectra containing solely the harmonic emission were observed. These spectra were obtained at the FP:SP ratios varied in the range of 0.3:1 and 4:1. This fact means that the favorable conditions for "optimal" plasma formation were mostly defined by the properties of microparticles rather than by the threshold of ablation of the sugar powder. The same can be said, to some extent, about the coffee powder.

Below we discuss the application of the double-pulse method for the nanoparticle targets. The ablation of nanoparticle (as well as microparticle) targets in our case could be as follows. The material surrounding nanoparticles is polymer (epoxy glue), which has a lower ablation threshold than metallic materials. The polymer starts to ablate at relatively low intensities of heating radiation, by carrying the nanoparticles out of the surface. The availability of various nanoparticles allows the formation of the laser-produced plasmas containing large amount of these species.

We analyzed the harmonic generation using the 802 nm double femtosecond pulses propagated close to the graphene nanoparticle contained target. Graphene nanoparticle powder (SkySpring Nanomaterials Inc.) was used as the ablating target. The graphene nanoparticles were presented in a broad range of sizes (10–80 nm) and had the shapes of the monolayer, bilayer, trilayer, etc. nanosized chunks, which represented the wrapped sheets of graphene. The powder of graphene nanoparticles was glued on the 5-mm-long glass plates and then installed in the vacuum chamber for ablation. We were able to achieve the conditions when the generating harmonics prevail over the plasma emission induced during ablation of graphene powder by the wings of the spatial distribution of the focused radiation. The optimum conditions were found at the FP:SP = 2:1 when the lower-order harmonics were generated while the plasma emission was insignificant.

The optimal distance between microparticle and nanoparticle contained surfaces and optical axis of femtosecond beam was larger compared with the case of solid targets ($d_{\mathrm{opt}} \approx$ 80–100 μm). The propagation of laser pulses through the plasma containing only glue molecules did not lead to harmonic generation using double-pulse scheme.

In these studies we observed the higher conversion efficiency for powdered targets compared with bulk solids. Note that well-known enhancement of conversion efficiency in the clustered media compared with monomer species of the same origin [16–28] has nothing common with our present meaning of the prevalence of the former media for HHG. In the above-refereed studies, the excellent features of clusters and metal or carbon nanoparticles were related with the mechanism of HHG, which has some advantages compared with monomer-induced HHG. Particularly, the comparative studies of HHG in the plasmas consisted of either nanoparticles or monomers showed that, at optimal experimental conditions of plasma

formation, the former species provide stronger harmonic yield, thus pointing out the advanced properties of the large emitters of harmonics in the nanoparticle-containing plasmas. The cross-section of recombination of the accelerated electron with the parent particle in the case of nanoparticles is higher compared with the atoms [25]. The uncertainty in the exact mechanism of the HHG from nanoparticles has previously been underlined in a few studies using gas clusters [25,29]. Among HHG mechanisms, the ionization and recombination to the same ion, to the neighboring ions, and to the whole nanoparticle have been proposed.

Contrary to that, in present studies, the prevalence of powdered species over bulk targets is related with the easiness in ablation and formation of plasma cloud prior to arrival of second pulse. This mechanism has nothing common with the above mechanisms. We just reiterate that the proposed scheme is more suitable for application of powdered materials. To add the proof for difference in the mechanisms of nanoparticle and/or cluster induced enhancement of harmonic efficiency reported so far and presented mechanism we just mention that both nano- and micro-particles are suitable for our approach, while previous studies have shown that the application of large particles (i.e. above a few tens nanometers) lead to a significant decrease of conversion efficiency compared with monomers due to some impeding processes, once equal plasma conditions become maintained in the case of delayed ablation of nano- and monomers.

We estimated the conversion efficiency of harmonics in the case of newly proposed scheme. Depending on target, it was 10 to 20 times smaller than the HHG conversion efficiency from the same samples at the optimal conditions of plasma formation. Particularly, as already mentioned the absolute value of conversion efficiency was calculated to be 1×10^{-6} in the case of double-pulse scheme using bulk silver target. In presented scheme, we did not pursue the amendment of HHG conversion efficiency, since it is obvious that the plasma formation conditions (e.g. plasma density, delay between heating and driving pulses, phase matching conditions, etc.) in that case were far from optimal compared with the conventional plasma harmonic scheme. We rather intended to show a new extremely simplified scheme of HHG allowing express-analysis of high-order nonlinear optical properties of a vast amount of solids, particularly, powdered materials.

4 Conclusions

Our studies of various materials using double-pulse method led to the following conclusions:

(i) Metal and non-metal bulk targets have demonstrated the weaker high-order harmonic generation compared with the more easily ablated powdered microparticle and nanoparticle species in the case of double-pulse method. The HHG in powders and nanoparticles was achieved in a much broader range of FP:SP ratios compared with the solids. The application of the powdered microparticle targets and nanoparticles glued on the glass substrates in the double-pulse scheme allowed the achievement of favorable conditions for the HHG. The heating, annealing, and evaporation of glued powders occurred at the conditions of stronger interaction of the target and the part of driving beam compared with the case of bulk targets.

(ii) The conditions of plasma formation and harmonic generation using double-pulse method in most cases were less favorable compared with the commonly used plasma harmonic method. Less suitable conditions of HHG in the case of double-pulse scheme decrease the efficiency of this process. One can assume the difficulty in the formation and maintenance of a sufficient amount of particles in the plasma plume produced during the excitation of the target by the part of the first pulse in the double-pulse scheme. Small delay between the FP and SP (8 ns) also prevents the appearance of the large amount of plasma species along the axis of propagation of the second pulse. This short delay between pulses did not allow the whole cloud of ablated particles reaching the optical axis of second pulse propagation where the intensity of laser radiation was maximal. Nevertheless, we were able observing the HHG even at these extremely unfavorable conditions.

References

1. F. Zernike, J.E. Midwinter, *Applied Nonlinear Optics* (Wiley, 1973)
2. J.F. Reintjes, *Nonlinear Optical Parametric Processes in Liquids and Gases* (Academic Press, 1984)
3. Y.R. Shen, *The principles of Nonlinear optics* (Wiley-Interscience, 2003)
4. Asselberghs, J. Perez-Moreno, K. Clays, in *Nonlinear Optical Properties of Matter: From Molecules to Condensed Phases*, edited by M.G. Papadopoulos, A.J. Sadlej, J. Leszczynski, Challenges and Advances in Computational Chemistry and Physics (2006), Vol. 1, p. 419
5. M.G. Humphrey, M.P. Cifuentes, M. Samoc, in *Molecular Organometallic Materials of Optics*, edited by H. LeBozec, V. Guerchais, Topics in Organometallic Chemistry (2010), Vol. 28, p. 57
6. S. Ghimire, A.D. DiChiara, E. Sistrunk, G. Ndabashimiye, U.B. Szafruga, A. Mohammad, P. Agostini, L.F. DiMauro, D.A. Reis, Phys. Rev. A **85**, 043836 (2012)
7. F. Kemper, B. Moritz, J.K. Freericks, T.P. Devereaux, New J. Phys. **15**, 023003 (2013)
8. S. Ghimire, A.D. DiChiara, E. Sistrunk, P. Agostini, L.F. DiMauro, D.A. Reis, Nature Phys. **7**, 138 (2011)
9. Y. Akiyama, K. Midorikawa, Y. Matsunawa, Y. Nagata, M. Obara, H. Tashiro, K. Toyoda, Phys. Rev. Lett. **69**, 2176 (1992)
10. R.A. Ganeev, M. Suzuki, S. Yoneya, H. Kuroda, Appl. Phys. Lett. **105**, 041111 (2014)
11. V. Strelkov, Phys. Rev. Lett. **104**, 123901 (2010)
12. McGuinness, M. Martins, P. Wernet, B.F. Sonntag, P. van Kampen, J.-P. Mosnier, E.T. Kennedy, J.T. Costello, J. Phys. B **32**, L583 (1999)

13. McGuinness, M. Martins, P. van Kampen, J. Hirsch, E.T. Kennedy, J.-P. Mosnier, W.W. Whitty, J.T. Costello, J. Phys. B **33**, 5077 (2000)
14. J.B. West, J.E. Hansen, B. Kristensen, F. Folkmann, H. Kjeldsen, J. Phys. B **36**, L327 (2003)
15. Y. Pertot, S. Chen, S.D. Khan, L.B. Elouga Bom, T. Ozaki, Z. Chang, J. Phys. B **45**, 074017 (2012)
16. T.D. Donnelly, T. Ditmire, K. Neuman, M.D. Pery, R.W. Falcone, Phys. Rev. Lett. **76**, 2472 (1996)
17. J.W.G. Tisch, T. Ditmire, D.J. Fraser, N. Hay, M.B. Mason, E. Springate, J.P. Marangos, M.H.R. Hutchinson, J. Phys. B **30**, L709 (1997)
18. T. Tajima, Y. Kishimoto, M.C. Downer, Phys. Plasmas **6**, 3759 (1999)
19. S.V. Fomichev, D.F. Zaretsky, D. Bauer, W. Becker, Phys. Rev. A **71**, 013201 (2005)
20. P. Moreno, L. Plaja, L. Roso, Europhys. Lett. **28**, 629 (1994)
21. S.X. Hu, Z.Z. Xu, Appl. Phys. Lett. **71**, 2605 (1997)
22. Vozzi, M. Nisoli, J.-P. Caumes, G. Sansone, S. Stagira, S. De Silvestri, M. Vecchiocattivi, D. Bassi, M. Pascolini, L. Poletto, P. Villoresi, G. Tondello, Appl. Phys. Lett. **86**, 111121 (2005)
23. C.-H. Pai, C.C. Kuo, M.-W. Lin, J. Wang, S.-Y. Chen, J.-Y. Lin, Opt. Lett. **31**, 984 (2006)
24. M. Kundu, S.V. Popruzhenko, D. Bauer, Phys. Rev. A **76**, 033201 (2007)
25. H. Ruf, C. Handschin, R. Cireasa, N. Thiré, A. Ferré, S. Petit, D. Descamps, E. Mével, E. Constant, V. Blanchet, B. Fabre, Y. Mairesse, Phys. Rev. Lett. **110**, 083902 (2013)
26. L.B. Elouga Bom, Y. Pertot, V.R. Bhardwaj, T. Ozaki, Opt. Express **19**, 3077 (2011)
27. Y. Pertot, L.B. Elouga Bom, V.R. Bhardwaj, T. Ozaki, Appl. Phys. Lett. **98**, 101104 (2011)
28. H. Singhal, P.A. Naik, M. Kumar, J.A. Chakera, P.D. Gupta, J. Appl. Phys. **115**, 033104 (2014)
29. V. Véniard, R. Taïeb, A. Maquet, Phys. Rev. A **65**, 013202 (2001)